

Generation of an Internal Fire Whirl in an Open Roof Vertical Shaft Model with a Single Corner Gap

G.W. Zou

College of Aerospace and Civil Engineering
Harbin Engineering University
Harbin, Heilongjiang, China

and

W.K. Chow*

Research Centre for Fire Engineering
Department of Building Services Engineering
The Hong Kong Polytechnic University
Hong Kong, China

*Corresponding author:

Fax: (852) 2765 7198; Tel: (852) 2766 5843;

Email: beelize@polyu.edu.hk; bewkchow@polyu.edu.hk

Postal address: Department of Building Services Engineering, The Hong Kong Polytechnic University, Hunghom, Kowloon, Hong Kong

Submitted: November, 2014

Revised: January, 2015

Abstract

An internal fire whirl (IFW) can be generated by burning a pool fire in a vertical shaft with appropriate sidewall ventilation provision. Earlier experimental results show that **the** flame swirling motion depends on the corner gap width providing ventilation. In this paper, experiments on generating an IFW in a 9 m tall vertical shaft model will be reported. Flame shapes in burning a gasoline pool fire inside the shaft model with different corner wall gap widths and tray diameters were observed. Fuel mass of the pool fire, flame height of the IFW, and transient air temperatures were measured.

From the results, it is further confirmed that an IFW cannot be generated **when the** gap width is too wide or too narrow. An IFW is developed in five stages. The pool fire is burning in a way similar to burning in open air at stage I. The burning rate of pool fire increases at stage II. Swirling flame motion starts to develop at stage III. An IFW develops fully at stage IV. Stage V is the decay stage. Further, the created IFW can be divided into three zones. Zone I is at the lower part with the flame rotating violently. Zone II is in the middle part with a slower swirling rate. The upper part zone III has no flame rotation.

Keywords: Fire whirl; Vertical shaft; Heat release rate; Flame height

Nomenclature

A_{Fire}	area of fuel tray, m^2
d	width of sidewall corner gap, m
D	diameter of fuel tray, m
f_h	flame height, m
f_m	mean flame height, m
ΔH_c	heat of combustion, kJ/kg
$\Delta H_{c,\text{eff}}$	effective heat of combustion, kJ/kg
$k\beta$	empirical constant, m^{-1}
m	transient fuel mass, kg
\dot{m}''	mass burning rate of fuel per unit surface area, $\text{kg}/(\text{m}^2 \cdot \text{s})$
\dot{Q}	heat release rate, kW
t	time, s
t_B	burning duration, s
z	height above fuel tray, m

1. Introduction

Fire whirls observed in big fires [1,2] can release high amounts of heat within a short time. More fuel was burnt with higher temperatures. A vortex similar to a tornado was formed with the burning fuel moving up as a spiral to give a swirling flame. Associated works on fire whirls in buildings had been studied extensively in the literature [3-18] focusing on understanding the generation mechanism and flow structure. An external source of angular momentum is required to produce buoyant whirls with large swirl velocity components while entraining air to the flame [1-5]. An internal fire whirl (IFW) can be created in a vertical shaft for tall buildings with appropriate sidewall ventilation provision [10,12,13,18]. It is very dangerous for firefighters staying nearby. The extended flame height will cause severe damage. In fire hazard assessments for tall shafts, rooms with ceiling vent and ventilation duct of green buildings, the scenario with an IFW should be included.

An ideal fire whirl model was presented by Chuah and Kushida [7] from experimental and numerical calculation to predict the flame heights and shapes of small fire whirls. The flame height of an IFW was found to be a function of the volume fuel rate which depended on the flame temperature and the vortex core radius. Swirling motion of an IFW was simulated by McDonough and Loh [5] with Computational Fluid Dynamics (CFD). A room-size enclosure buoyant whirling flame was reported by Snegirev et al. [6]. The periodic formation and destruction of the whirling core, and the increase of the time-averaged burning rate were observed. Experimental and numerical results comparison with similarity analysis was reported by Kuwana et al. [19]. However, understanding of the mechanism of generating an IFW is still incomplete as raised by Chuah et al. [11]. More works are required for fire engineering application.

Laboratory-scale IFWs were studied by Dobashi and associates [15-17]. Tangential and radial velocity distributions near the flame base of an IFW generated by burning methanol pool fires were measured [15]. Changes in flame height and flame-base shape under three different flow conditions were studied to understand the flame height, vortex structure and the mechanism for elongating the flame height. The radial velocity distribution near the flame base would affect the flame height because the radial inflow would reduce the flame shape to give a higher heat flux to increase the evaporation rate of liquid fuel at the surface.

An IFW is said [16] to be weak when the pure aerodynamic effect of flow circulation has little effects on the flame length. Split cylinders were used to apply a flow circulation to a 3 cm diameter methane burner flame and a 3 cm diameter ethanol pool fire. After applying the flow circulation, the flame length of the ethanol pool fire increased about three times. The flame shape of the ethanol pool fire changed and gave higher heat to the fuel surface. The burning rate increased. The flame length of the methane burner flame did not change much because of its constant burning rate. Therefore, the flame length increased because of changing the burning rate even under a weak circulation condition. CFD simulations were conducted to understand the detailed flow structure of the fire whirl. An analytical model was then developed based on the experimental observations and CFD simulations. The predicted relationship between the flame height and the burning rate agreed well with experimental data.

The burning rate of an IFW depends on the nature of the vortex. Flame height of an IFW should be able to be expressed as a function of vortex parameters, specifically, the circulation and the core radius of the vortex. A flame height correlation [17] can be derived through experiments, CFD simulation, and theoretical analysis.

In this paper, the effect of sidewall ventilation provision [10,12,13,18] on creating an IFW in a 9 m tall vertical shaft will be further investigated.

2. Full-scale Burning Tests

Experiments on IFW were carried out in a typical vertical 2.1 m square shaft model of height 9 m [12] in a large burning hall in China. The model was constructed by a steel framework with galvanized steel sheets of 1 mm thick with an open roof as shown in Fig. 1a. A vertical gap with adjustable gap width d was opened at one corner of the model. Ambient air induced by the burning fuel to the model swirled as in Fig. 2a. Two pieces of 4 mm thick glass sheets each of height 1.5 m were put at the front wall for observing the flame motion.

A liquid pool fire of different tray diameters D of 20 cm, 26 cm and 46 cm was placed at the center of the shaft model as in Fig. 1b. Gasoline 93# available in China was used in the experiments. The physical parameters of gasoline are [20]: heat of combustion 43070 kJ/kg (10300 kcal/kg), density from 700 kg/m³ to 790 kg/m³, latent heat of vaporization from 290 kJ/kg to 315 kJ/kg, and self-ignition point from 415°C to 530°C.

Two thermocouple trees TC1 and TC2 of type K bare wire of diameter 0.5 mm were put at the center and at the corner of the model as in Fig. 1a and 1b. Thermocouple tree TC1 as shown in Fig. 1c could be raised up or lowered down by a pulley to put the first thermocouple at the top edge of the fuel tray with different depths and diameters. The radial temperatures at 0 m, 1 m, 2 m above the top edge of the fuel tray were measured. The distance between two thermocouples in TC1 was 0.5 cm. There were 10 thermocouples on the corner tree TC2 spaced at intervals of 90 cm.

Fuel mass was measured by an electronic balance with a precision of 0.005 kg and a range of 75 kg. Signals of temperature were sampled once per second, and signals of fuel mass were sampled 15 times per second.

The burning process and flame development were recorded by a video recorder and camera. The size and geometry of the flames, such flame height and flame shape, were then read from the captured photographs.

Physical parameters on burning rate of the pool fire, the size and geometry of the flames, temperature distribution, velocity distribution, and air entrainment rate used for describing the flame intensity and IFW characteristics were measured in the tests.

Two sets of tests F1 and F2 with a summary of the experimental details shown in Table 1 were carried out:

- Test F1 on varying the corner gap width:

Eight tests labelled F1-1 to F1-8 were carried out with vertical gap widths d of 1.3 cm, 5.5 cm, 11 cm, 22 cm, 33 cm, 44 cm, 66 cm and 88 cm respectively. A pool fire of the same diameter D of 46 cm, 10 cm in depth and 3 liters gasoline was used in each test.

- Test F2 on varying the diameter of the fuel trays:

Three tests labelled F2-1, F2-2 and F2-3 were carried out with fuel tray diameters D of 20 cm, 26 cm and 46 cm respectively. The depths of fuel trays were 5 cm, 5 cm and 10 cm respectively. Volumes of gasoline used were 0.5 liter, 0.7 liters and 5 liters respectively. Value of d was kept at 33 cm.

Two trials of each test were carried out to better understand the generation mechanism and structure of the IFW in a vertical shaft model with one corner gap.

The effect of fuel tray depth on the generation of a fire whirl is not considered in this paper. Note that the burning rate of pool fires depends on the lip height affecting the turbulence close to the pool edge, the heat conduction of the vessel wall and flame radiation. Further, it was suggested [14] that lip height of fuel pool had little effect on the burning rate of a fire whirl.

3. Experimental Observations

An IFW was created with appropriate values of d . When the gasoline pool fire was ignited in the shaft model, the flame was similar to a pool fire burning in open air initially as indicated by the photographs taken at 5 s and 10 s in Fig. 2a. Several seconds later, the entrained air from the vertical gap was involved in the burning process at a **higher** position. The flame of the pool fire was disturbed by the entrained air. The flame shook vigorously, tilted and revolved around the geometrical central axis of the model from 20 s to 30 s as shown in Fig. 2a. However, the flame did not rotate by itself as in Fig. 2b. The angular speed of the flame revolution was increasing **with accelerated** burning. After a further period of time, the flame tip turned rapidly into the vertical axis and started to spin around the flame axis. This region of flame self-rotation shortly extended downward to the fuel surface, which was consistent with the observations of the formation of a concentrated vortex [14,**21,22**]. Finally, an IFW was formed with the flame **extending** along the vertical direction with rapid rotation as shown in the photographs captured at 66 s and 73 s in Fig. 2a. The flames

revolved about the central axis of the pool tray in all tests with a curved shape, but did not appear as a vertical cone along the central axis as observed by others [1,14,21].

To compare the burning of the pool fire in open air with that in the vertical shaft model, two pools of the same tray diameter of 0.2 m and same amount of fuel were set up as in Fig. 3 and ignited at the same time. The flame height in the model is much higher than that in open air with some results shown in Fig. 3. An IFW appeared in the vertical model with a large height to diameter ratio. Rotating airflow motion was not observed in the pool fire burning outside.

The created IFW did not orientate about a vertical axis. The lower part of the flame was vertical, but the upper part of the flame was tilted as in Fig. 2c and Fig. 3. The central axis of the upper part of the IFW was not orientated vertically as a pool fire burning in open air. The flame rotated quickly about its own axis, but the flame axis swirled about the central vertical axis of the pool tray to give flame ‘wandering’ or ‘precession’.

An axisymmetric turbulent fire plume can be divided into three zones [23] as shown in Fig. 4a. By observing the fire flame pictures taken from the experiments as in Fig. 4b, Table 2 for tests F1 and Table 3 for tests F2, three distinct zones can also be divided for an IFW in the square vertical shaft with a sidewall corner gap as in Fig. 4c:

- Zone I with violently rotating flame:

Zone I is located at the lower part of the IFW with the flame swirled vigorously. A helical upward motion was observed. The flame had a bright colour without spreading out.

- Zone II on flame transition:

Zone II is at the middle part of the IFW with the flame swirled slowly. The helical motion stretched by a longer distance. Flame colour was yellow and became darker.

- Zone III without rotating flame:

Zone III is located at the top of the IFW with the flame swirled. The flame jumped up, stretched as a curve shape with varying shapes. Flame colour turned red.

Vertical temperature profiles **T at the centerline** at different heights z above the ground for test F2-3 are plotted in Fig. 4d. The temperature profiles can be divided into three distinct zones due to flame swirling. The highest temperature was measured in zone I, and the lowest temperature measured in zone III. Flame temperature at centerline increased with height in zone I, and then dropped rapidly. At zone II, the temperature began to increase slowly. In zone III, the temperature started to decrease.

The burning process of the pool fire and flame development in the IFW were recorded by a digital video recorder and camera. The transient flame heights f_h over time in the experiments were read directly from the captured photographs as reported before [13]. Pictures of flames were taken from the video recorded at intervals of 1 s to measure the flame height. An example of the transient flame height f_h at time t for test F2-3 (D of 46 cm and d of 33 cm) is shown in Fig. 5. The mean flame height f_m of the IFW was 3.3 m.

4. Development of an IFW

Typical curves on transient temperature at different heights and fuel mass of the pool fire for tests F2-3 when an IFW was created in the vertical shaft model are shown in Fig. 6. For test F2-3, d was 33 cm, D was 46 cm with 5 liters gasoline. The test was repeated twice with results on the fuel mass change with time shown in Fig. 6a and centerline temperature change with time in Fig. 6b. Flame temperatures at centerline were measured at heights 0.1 m, 1 m, 2 m from the top edge of the fuel tray.

The initial masses of gasoline were 3.56 kg and 3.54 kg respectively in the two tests of F2-3. Density of gasoline was 710 kg/m^3 , calculated from the mass 3.55 kg and volume 5 liters. It is shown from Fig. 6 on transient fuel mass m at different time t that fuel mass dropped and air temperatures rose during the burning process. When the fuel tray was ignited, flame temperature at z of 0.1 m rose suddenly as shown in Fig. 6b. Air temperatures rose suddenly at about 170 s. As observed, the creation of an IFW started. In the period from 200 s to 280 s, an IFW was created with flame rotating. After 280 s, air temperatures began to decrease, and fuel was gradually consumed out. Note that the fuel masses were measured by the strain gauge in the electric balance. Negative mass values might suggest a strong upward pull such as suction in a tornado was created by the IFW. Suction force appears when fire whirl occurs. When the IFW was weakened, the fuel mass curve began to rise. When burning terminated, buoyancy and pull force disappeared and hence, the electronic balance reading returned back to 0 kg.

It can be seen from Fig. 6 that, based on the change of temperature and mass, the entire burning process can be divided into five stages. From the transient curves of fuel mass shown

in Fig. 6a, each stage has a different slope. It means that each stage has a different fuel consumption rate.

- Stage I:

The first stage is similar to a general pool fire in open air. The fuel consumption rate was about 0.0103 kg/s or 0.0620 kg/(m² · s).

- Stage II:

The second stage has a faster burning rate of pool fire. The fuel consumption rate was 0.0144 kg/s or 0.0867 kg/(m² · s).

- Stage III:

Swirling motion starts to develop at this stage.

- Stage IV:

Stage four is the development stage of fire whirl. The fuel consumption rate was 0.0192 kg/s or 0.1156 kg/(m² · s).

- Stage V:

This is the decay stage of fire whirl.

The fuel consumption per unit area with an IFW is almost 2 times that in an open air pool fire. The transient fuel mass curves in Fig. 6a also showed that an IFW has a long burning duration with a constant burning rate of fuel mass, indicating that the IFW is very stable. However, it took a long time about 180 s for test F2-3 to achieve this steady burning rate.

Repeatability should be watched in experiment. As seen from Fig. 6, the results of each test with two trial runs indicated good repeatability on transient fuel masses and air temperatures T at 0.1 m, 1 m and 2 m above the fuel tray.

5. Results of Tests F1

The effect of varying the corner gap width on the creation of an IFW in tests F1-1 to F1-8 is summarized in Table 2. It is observed that the flame shape changed with different values of d .

As shown in the table, air intake to the shaft model depends on the value of d . Supplying more air from the sidewall would provide oxygen to burn the fuel moved up by swirling motion. However, supplying too much air would change the mixing ratio of fuel with air. Combustion process of fuel cannot be sustained and hence an IFW would not be created. On the other hand, small values of d would not give sufficient air to sustain combustion.

As shown in Table 2 for vigorous swirling motion of IFW, the mean flame height became taller. The pool fire had faster burning rates. The mean flame height was stretched to double the normal value.

Fig. 7 shows the transient burning duration t_B and the mean flame height f_m curves at different vertical gap widths as summarized in Table 2. It is observed that a strong fire whirl can be created when d is between 0.2 m to 0.5 m.

6. Results of Tests F2

The effect of varying the fuel tray diameter D of the three tests F2-1, F2-2 and F2-3 on the creation of an IFW was studied in tests F2. The corner gap width d of the shaft model was different. A summary is shown in Table 3. The vertical temperature profiles T at different heights above the fuel tray z measured by TC1 at the central pool axis of the model are shown in Fig. 8.

As observed, for D of 46 cm, the IFW induced was very strong. This can be illustrated by the flame height and vertical temperature profile.

A pool fire with a bigger tray diameter would give a higher heat release rate and hence stronger buoyancy of hot gases moving up. More fuel was evaporated from the pool tray to give a hotter and longer flame.

7. Heat Release Rate Estimation

Heat release rate (HRR) is an important parameter on fire development and is commonly used to correlate the flame height of pool fire [23,24]. HRR is not a fundamental property of a fuel and so cannot be calculated from the basic material properties. It depends on how the fuel is burnt and so is usually determined from experimental measurement such as the oxygen consumption calorimetry [25]. As seen in Fig. 6a, burning rates can be calculated from the transient mass curves by neglecting the upward pull of the IFW. However, the heat release rates were difficult to estimate from the mass loss rate curves.

The HRR of the gasoline pool fire of diameter D of 46 cm was measured by the oxygen consumption calorimetry. Three cases were considered with cases 1 and 2 on burning the pool fires in open air, and case 3 on confined pool fire.

- Case 1: 2 liters gasoline with the fuel tray put below the exhaust hood.
- Case 2: 3 liters gasoline with the fuel tray put below the exhaust hood.
- Case 3: 4 liters gasoline with the fuel tray put at the corner of the room calorimeter [26].

Results of HRR are shown in Fig. 9. The peak HRR values were 200 kW in case 1, 225 kW in case 2, and 350 kW in case 3. The HRR of the pool fire in open air is almost the same for cases 1 and 2, but smaller than the HRR measured in the room. Compartment boundary surfaces radiate heat toward the fuel surface, thereby increasing the fuel burning rate.

If the area of the fuel tray and effective heat of combustion are known, the HRR of pool fire \dot{Q} of fuel tray diameter D can be calculated [23,24] by the mass burning rate of fuel per unit surface area \dot{m}'' , the effective heat of combustion $\Delta H_{c, \text{eff}}$, empirical constant $k\beta$, and surface area of pool fire A_{Fire} (area involved in vaporization):

$$\dot{Q} = \dot{m}'' \Delta H_{c, \text{eff}} (1 - e^{-k\beta D}) A_{\text{Fire}} \quad (1)$$

For a large pool of D over 0.2 m, relevant data reported [23,27] for gasoline pool fires are $\dot{m}'' = 0.055 \text{ kg}/(\text{m}^2 \cdot \text{s})$, $\Delta H_{c, \text{eff}} = 43700 \text{ kJ/kg}$ (higher than heat of combustion $\Delta H_c = 43070 \text{ kJ/kg}$ used in experiment) and $k\beta = 2.1 \text{ m}^{-1}$. For a pool tray with D of 46

cm, $A_{\text{Fire}} = 0.1661 \text{ m}^2$. The estimated heat release rate of the pool fire in open air was 247.3 kW, matching with the measured value 225 kW in case 2.

Using burning rate \dot{m}'' of $0.055 \text{ kg}/(\text{m}^2 \cdot \text{s})$ and measured value \dot{Q} of 225 kW, the effective heat of combustion of gasoline used in the experiment was estimated to be 39800 kJ/kg by equation (1). A summary of results on cases 1 to 3 is shown in Table 4.

The transient fuel mass at the different stages of an IFW in test F2-3 were measured as shown in Fig. 6a. Values of the burning rates per unit surface area \dot{m}'' are $0.0620 \text{ kg}/(\text{m}^2 \cdot \text{s})$ in stage I, $0.0867 \text{ kg}/(\text{m}^2 \cdot \text{s})$ in stage II, and $0.1156 \text{ kg}/(\text{m}^2 \cdot \text{s})$ in stage IV, respectively. Substituting these measured values \dot{m}'' at different stages together with $\Delta H_{c, \text{eff}} = 39800 \text{ kJ/kg}$ and $k\beta = 2.1 \text{ m}^{-1}$ into equation (1), the HRR of test F2-3 at different stages are estimated and shown in Table 4.

The HRR values are 253.9 kW, 355.0kW, and 473.4 kW respectively. The HRR 253.9 kW in stage I is consistent with the measured value 225 kW for cases 1 and 2 under the exhaust hood and the estimated value 243.7 kW by equation (1). Results indicated that stage I is similar to a pool fire burning in open air. At stage II, the burning rate of fuel was much faster. Stage IV had a stable IFW with HRR of 473.4 kW, twice the value of 225 kW for burning the same pool fire in open air.

8. Conclusions

Experiments on generating an IFW by burning a gasoline pool fire in a vertical shaft with an open roof were carried out. The following conclusions are drawn:

- An IFW was observed by burning a gasoline pool fire at the center of the model with a single corner gap at one sidewall. Different gap widths at the corner would give different circulation air flow in the shaft model. Therefore, an IFW could not be onsetted when the gap width was too wide or too narrow.
- Generation of an IFW is developed in five stages. The pool fire is burning in a way similar to burning in open air at stage I. The burning rate of pool fire increases at stage II. Swirling flame motion starts to develop at stage III. An IFW develops fully at stage IV. Stage V is the decay stage.
- The generated IFW has three zones. Zone I is at the lower part with the flame rotating violently. Zone II is in the middle part with a slower swirling rate. The upper part zone III has no flame rotation.

Fire whirls generated in an open field were classified by Soma and Saito [28] into three prototypes with two on 'moving-type' and one as 'stationary-type'. Generation mechanism of the open type fire whirls spun about the centre without any surrounding walls appears to be similar to the generation of the IFW for an open roof vertical shaft model. Therefore, the air flow resulted from a narrow region between the horizontal wind speed and the heat generating source of the open type fire whirls would give some hints on further studying the effect of different slit widths on generating an IFW in this study.

Funding

This work described in this paper was supported by a grant from the Research Grants Council of the Hong Kong Special Administrative Region, China for the project “A study of internal fire whirl in vertical shafts with open roofs” with project number: 513713.

References

1. Emmons HW and Ying SJ. The fire whirl. In: *Proceedings of the 11th International Symposium on Combustion*, 1967, pp. 475-488. Pittsburgh, PA: Combustion Institute.
2. Meroney RN. Fires in porous media: natural and urban canopies. In: Gayev YeA and Hunt JCR (eds) *Flow and Transport Processes with Complex Obstructions*. Springer, 2007, Chapter 8, pp. 271-310.
3. Battaglia F, McGrattan KB and Rehm RG et al. NISTIR 6341:1999. Simulating fire whirls. National Institute of Standards and Technology, USA.
4. Satoh K and Yang KT. Measurements of fire whirls from a single flame in a vertical square channel with symmetrical corner gaps. In: *1999 ASME International Mechanical Engineering Congress and Exposition*, Nashville, TN, 14-19 November 1999, ASME HTD-Vol. 364-4, pp.167-173.
5. McDonough JM and Loh A. Simulation of vorticity-buoyancy interactions in fire-whirl-like phenomena. In: *Proceedings of HT2003 ASME Summer Heat Transfer Conference*, Las Vegas, Nevada, USA , 21-23 July 2003.
6. Snegirev AY, Marsden JA and Francis J et al. Numerical studies and experimental observations of whirling flames. *Int. J. Heat Mass Transfer*, 2004; 47: 2523-2539.
7. Chuah KH and Kushida G. The prediction of flame heights and flame shapes of small fire whirls. *Proc. Combust. Inst.* 2007; 31: 2599-2606.
8. Zhou R and Wu ZN. Fire whirls due to surrounding flame sources and the influence of the rotation speed on the flame height. *J. Fluid Mech.* 2007; 583: 313-345.
9. Kuwana K, Sekimoto K and Saito K et al. Scaling fire whirls. *Fire Safety J.* 2008; 43(4): 252-257.

10. Chow WK and Han SS. Experimental investigation on onsetting internal fire whirls in a vertical shaft. *J. Fire Sci.* 2009; 27(6): 529-543.
11. Chuah KH, Kuwana K and Saito K. Modeling a fire whirl generated over a 5-cm-diameter methanol pool fire. *Combust. Flame* 2009; 156: 1828-1833.
12. Zou GW, Yang L and Chow WK. Numerical studies on fire whirls in a vertical shaft. In: *2009 US-EU-China Thermophysics Conference-Renewable Energy (UECTC-RE '09)*, Beijing, China, 28-30 May 2009.
13. Chow WK, He Z and Gao Y. Internal fire whirls in a vertical shaft. *J. Fire Sci.* 2011; 29(1): 71-92.
14. Lei J, Liu NA and Zhang LH, et al. Experimental research on combustion dynamics of medium-scale fire whirl. *Proc. Combust. Inst.* 2011; 33: 2407-2415.
15. Hayashi Y, Kuwana K and Dobashi R. Influence of vortex structure on fire whirl behavior. In: *Fire Safety Science – Proceedings of 10th International Symposium*, University of Maryland, USA, 19-24 June 2011, pp. 671-680.
16. Kuwana K, Morishita S and Dobashi R, et al. The burning rate's effect on the flame length of weak fire whirls. *Proc. Combust. Inst.* 2011; 33: 2425-2432.
17. Hayashi Y, Kuwana K and Mogi T et al. Influence of vortex parameters on the flame height of a weak fire whirl via heat feedback mechanism. *J. Chem. Eng. Japan* 2013; 46(10): 689-694.
18. Chow W.K. A study on relationship between burning rate and flame height of internal fire whirls in a vertical shaft model. *J. Fire Sci.* 2014; 32(1): 72-83.
19. Kuwana K, Hassan M, Wang F and Saito K. Flow and temperature structures of a fixed-frame type fire whirl. In: *Fire Safety Science – Proceedings of the Eighth International Symposium*, International Association for Fire Safety Science, 2005, pp. 951-962.

20. GB/T 2589-2008. General principles for calculation of the comprehensive energy consumption. National Standards of the People's Republic of China, 2008.
21. Lei J, Liu NA and Lozano JS et al. Experimental research on flame revolution and precession of fire whirls. *Proc. Combust. Inst.* 2013; 34: 2607-2615.
22. Zhou KB, Liu NA and Lozano J.S. et al. Effect of flow circulation on combustion dynamics of fire whirl. *Proc. Combust. Inst.* 2013; 34: 2617-2624.
23. Karlsson B and Quintiere JG. *Enclosure fire dynamics*. CRC Press, 2000.
24. Lei J, Liu NA and Zhang LH et al. Burning rates of liquid fuels in fire whirls. *Combust. Flame* 2012; 159: 2104-2114.
25. Iqbal N, Salley MH and Weerakkody S. et al. Fire Dynamics Tools (FDTs): Quantitative fire hazard analysis methods for the U.S. nuclear regulatory commission fire protection inspection program. NUREG-1805, December 2004.
26. ISO 9705. Fire tests — Full-scale room test for surface products, 1st ed., 1993-06-15, Corrected and reprinted 1996-03-01. International Organization for Standardization, Geneva.
27. Babrauskas V. Burning rates. In: DiNenno PJ (ed) *SFPE Handbook of Fire Protection Engineering*. 3rd ed. National Fire Protection Association, Quincy, Massachusetts, 2002, Section 3, Chapter 3-1.
28. Soma S and Saito K. Reconstruction of fire whirls using scale models. *Combust. Flame* 1991; 86: 269-284.

JFS_ZouIFW141w

Author Biographies

G.W Zou is an Associate Professor at the College of Aerospace and Civil Engineering, Harbin Engineering University, Harbin, Heilongjiang, China. His main research interests are on fire safety assessment on computational fluid dynamics in fire engineering, flammable materials in building materials and fire test design. Over 30 papers have been published in journals and conference proceedings.

W.K. Chow is the Chair Professor of Architectural Science and Fire Engineering, Director of Research Centre for Fire Engineering, and Head of Department, Department of Building Services Engineering of The Hong Kong Polytechnic University. He is the Founding President of the Hong Kong Chapter, Society of Fire Protection Engineers since 2002; and President of the Asia-Oceania Association for Fire Science and Technology since 2007. He was elected as a Fellow of the Hong Kong Academy of Engineering Sciences in 2012; and appointed to be a Justice of **the** Peace by the Chief Executive of the Hong Kong Special Administrative Region in 2013.

List of Figures

Fig. 1: The vertical shaft model

Fig. 2: Flame images of transition from a general pool fire to a fire whirl

Fig. 3: Pool fires burning in open air and in the vertical shaft for test F2-1

Fig. 4: Pool fires in open air and IFW in a vertical shaft

Fig. 5: Transient flame heights for test F2-3

Fig. 6: Transient fuel mass and centerline temperatures at different heights for test F2-3

Fig. 7: Burning duration and mean flame height curves for different gap widths

Fig. 8: Vertical temperature profiles at center for tests F2

Fig. 9: Heat release rate measured by oxygen consumption calorimetry

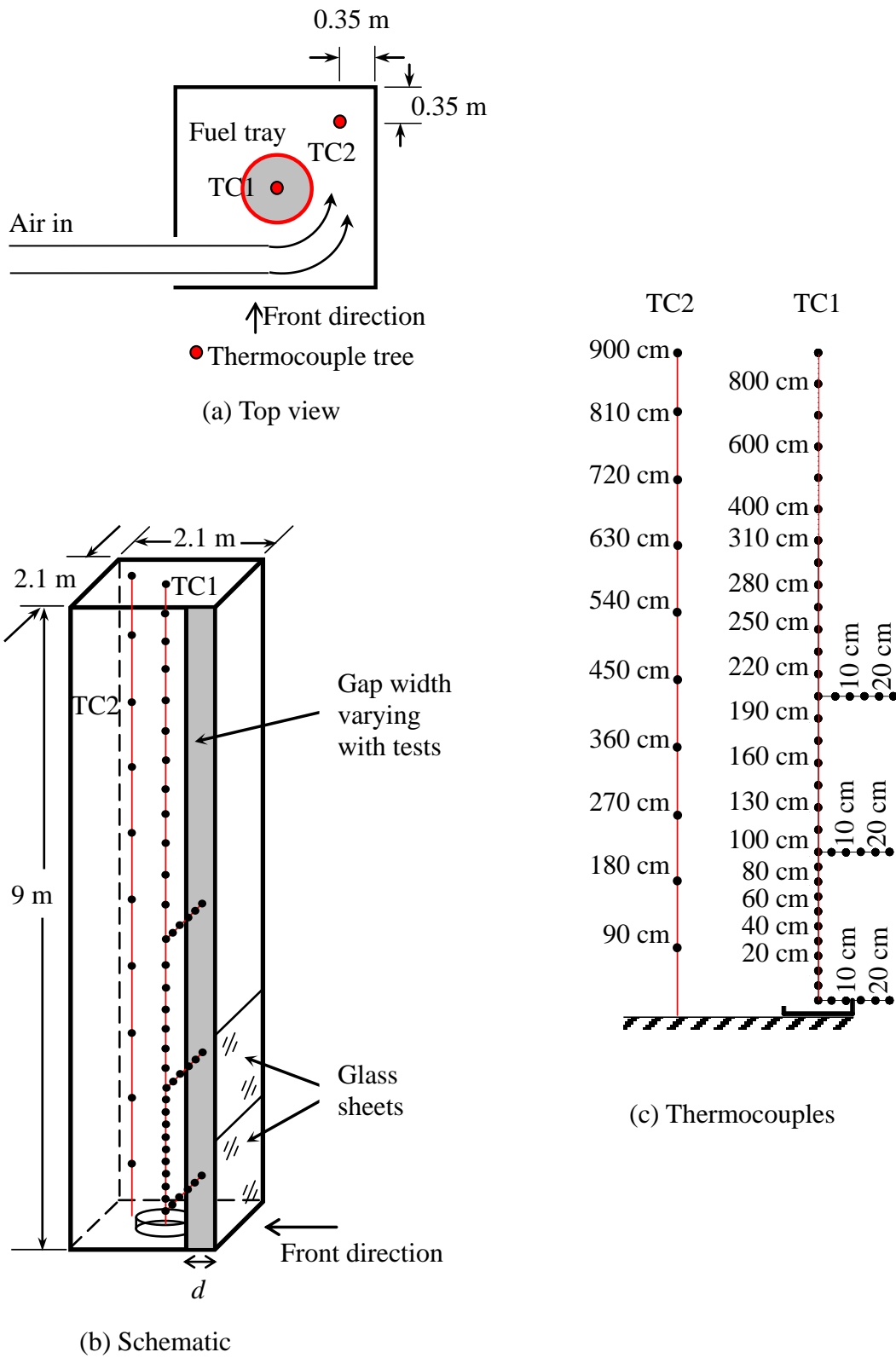
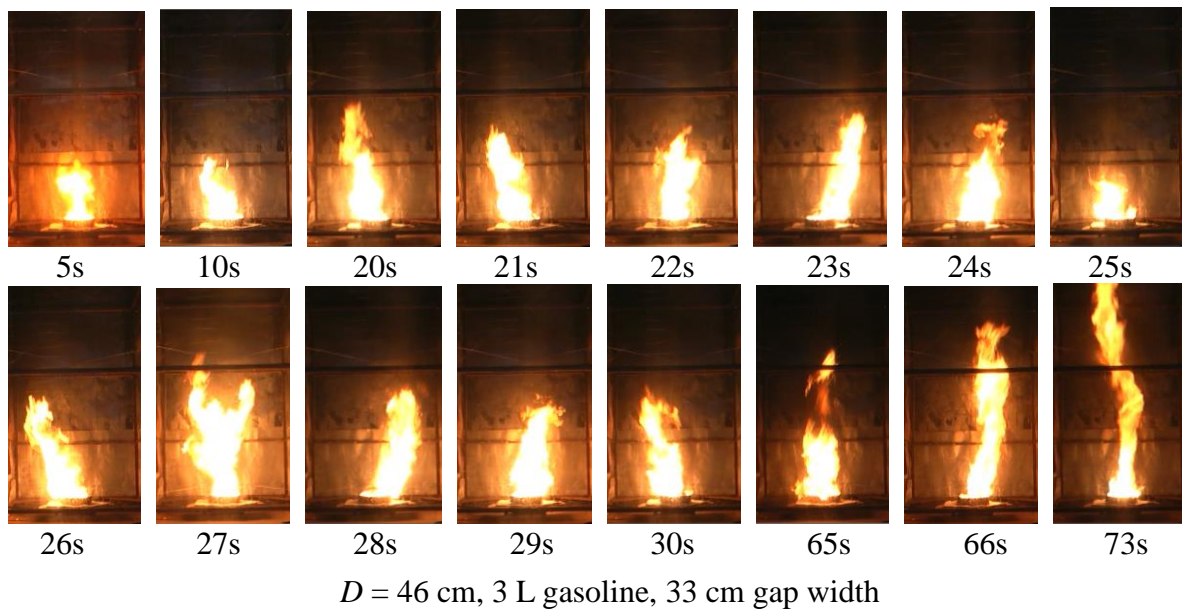


Fig. 1: The vertical shaft model



(a) Flame shapes sequence of test F1-5

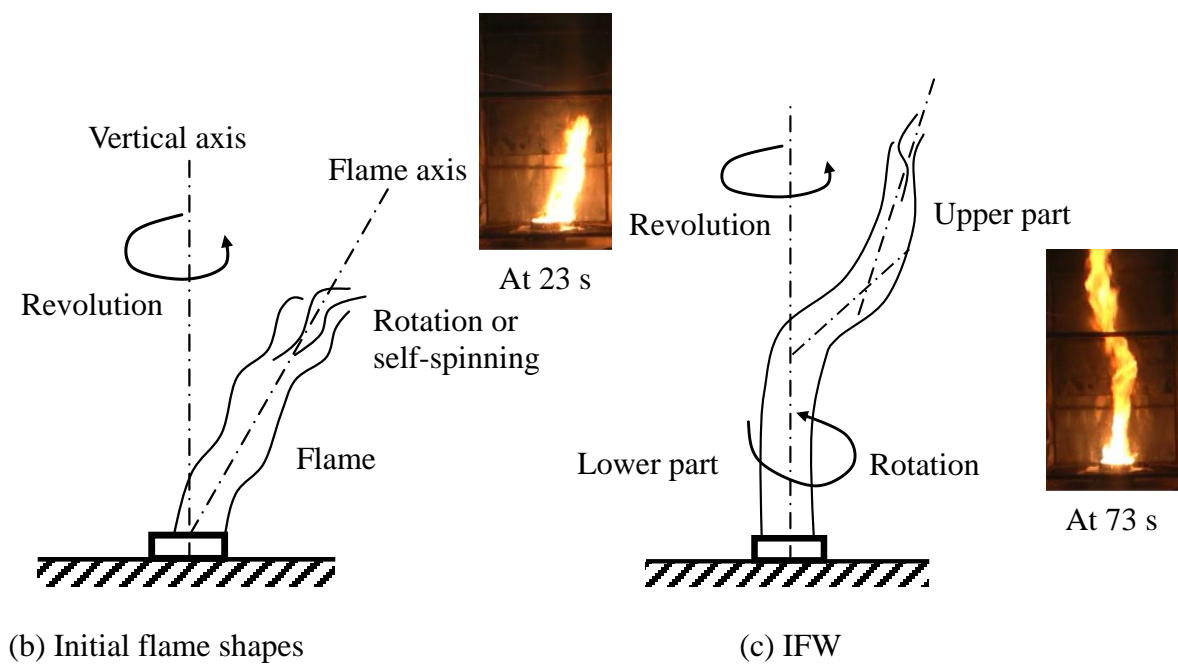
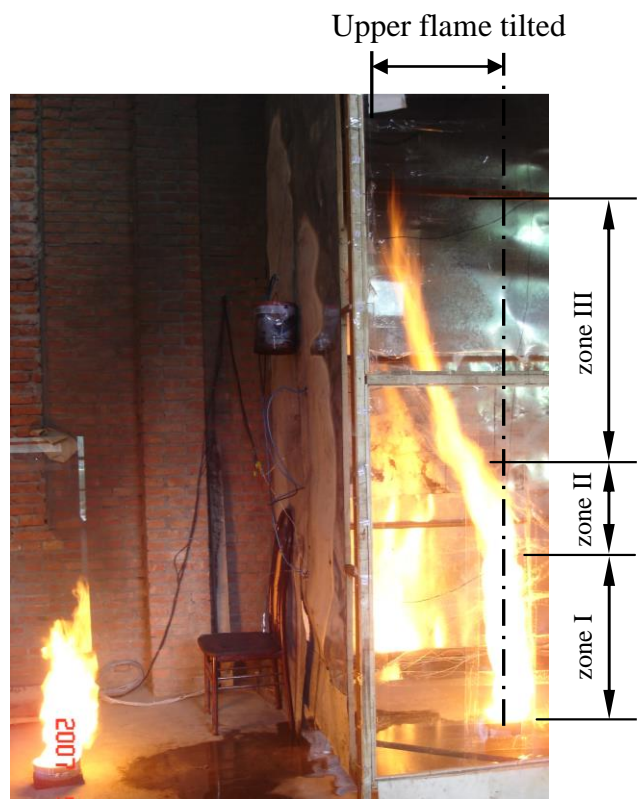
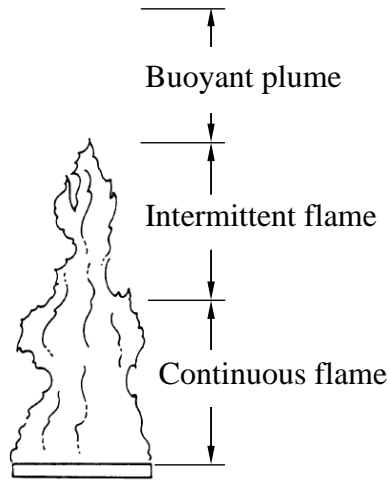


Fig. 2: Flame images of transition from a general pool fire to a fire whirl

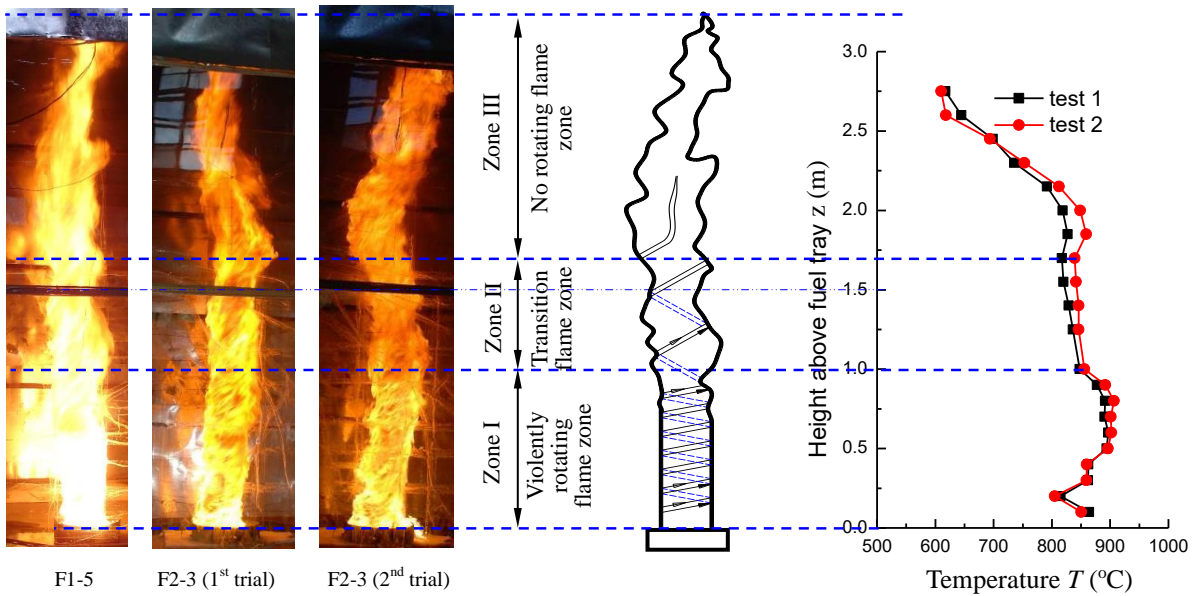


$D = 20$ cm, 0.5 L gasoline, 14 cm gap

Fig. 3: Pool fires burning in open air and in the vertical shaft for test F2-1



(a) Pool fire in open air



$D = 46$ cm, 33 cm gap width

(b) IFW

(c) Three zones

(d) Axial profiles of mean temperature for test F2-3

Fig. 4: Pool fires in open air and IFW in a vertical shaft

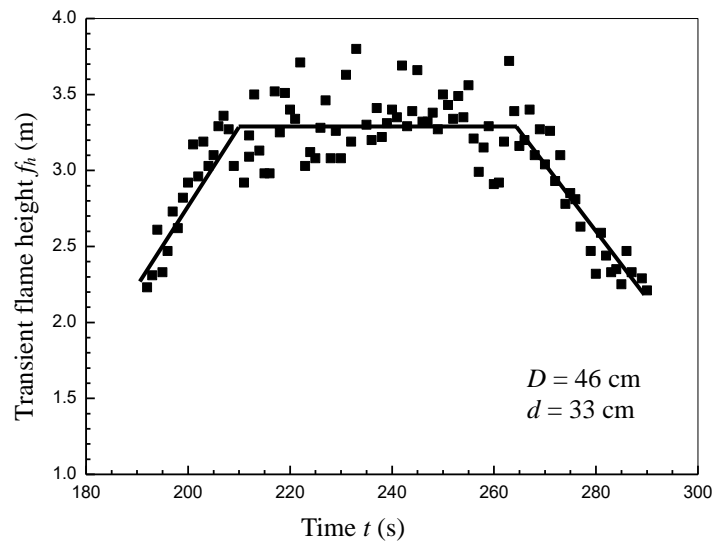
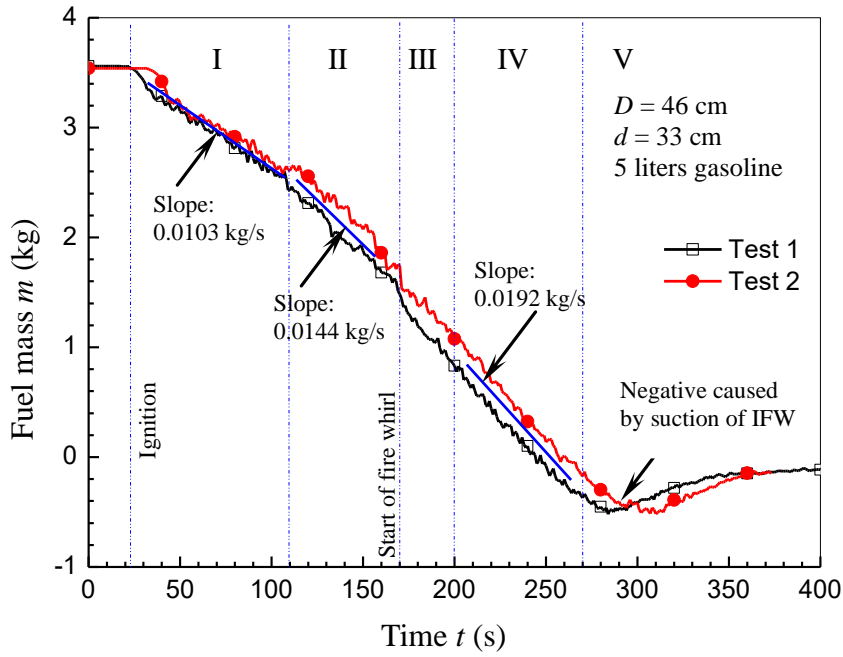
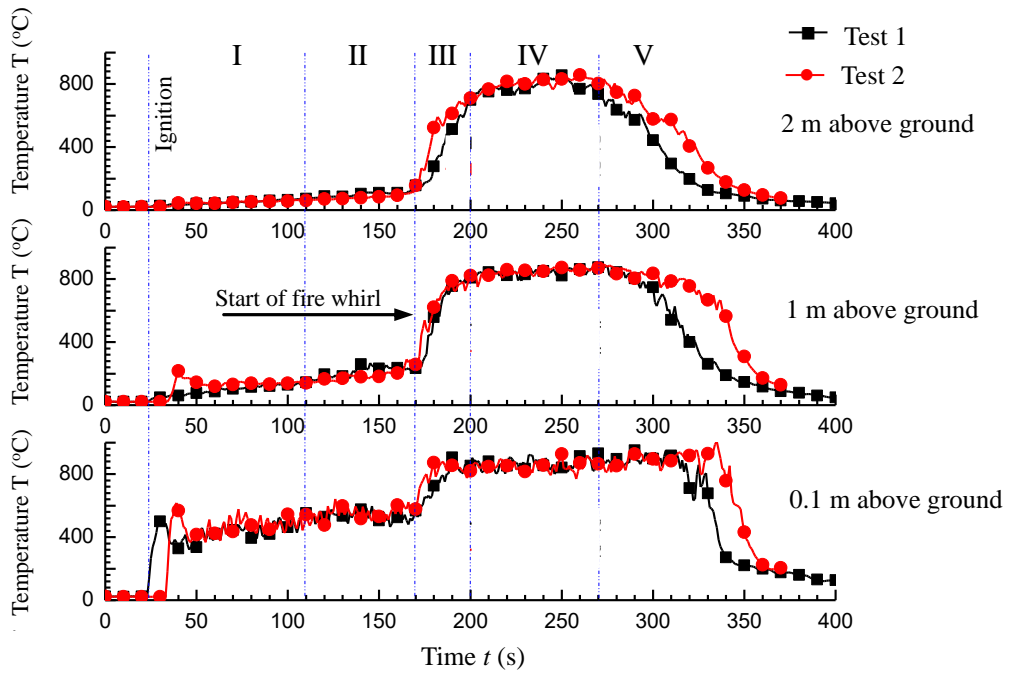


Fig. 5: Transient flame heights for test F2-3



(a) Transient fuel mass curves



(b) Transient centerline temperature at different heights

Fig. 6: Transient fuel mass and centerline temperatures at different heights for test F2-3

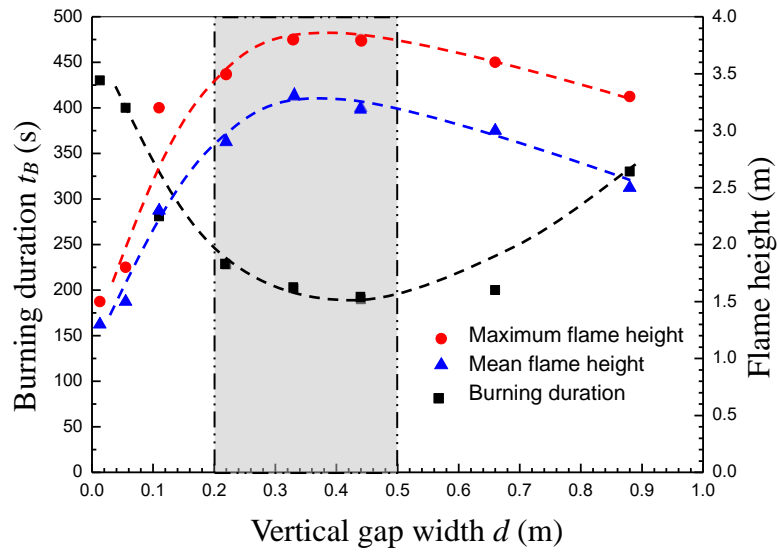


Fig. 7: Burning duration and mean flame height curves for different gap widths

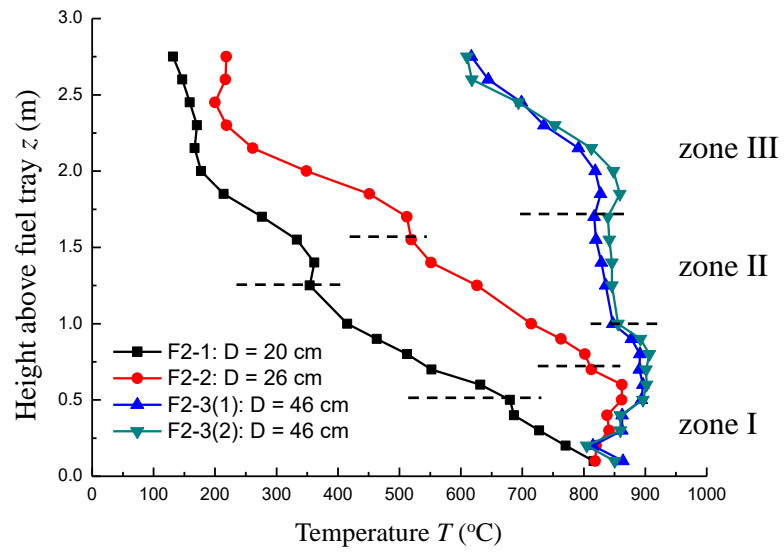


Fig. 8: Vertical temperature profiles at center for tests F2



Case 1



Case 2



Case 3

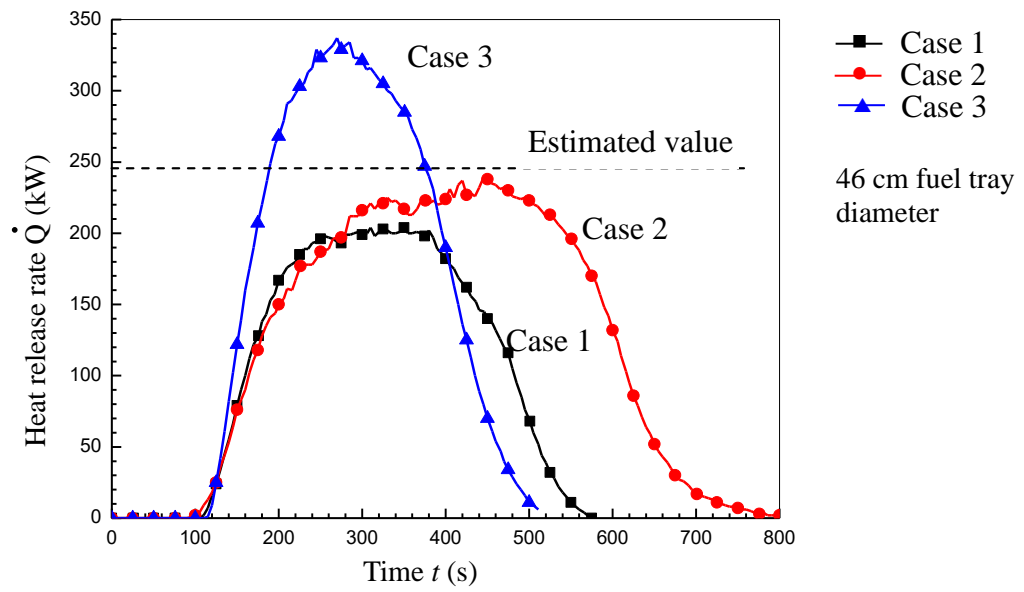


Fig. 9: Heat release rate measured by oxygen consumption calorimetry

List of Tables

Table 1: The two sets of tests

Table 2: Summary of tests F1

Table 3: Experiment results of the test F2 on varying the fuel tray diameter

Table 4: Estimation of heat release rates of IFW

Table 1: The two sets of tests

Test group	Test No.	Diameter of fuel tray D (cm)	Depth of fuel tray (cm)	Vertical gap d (cm)	Fuel volume (liters)	Mean flame height f_m (m)	Observation on IFW
F1: Varying the width of the corner gap	F1-1	46	10	1.3	3	1.3	No swirling
	F1-2	46	10	5.5	3	1.5	No swirling
	F1-3	46	10	11	3	2.3	Weak swirling
	F1-4	46	10	22	3	2.9	Moderate swirling
	F1-5	46	10	33	3	3.2	A clear IFW
	F1-6	46	10	44	3	3.1	A clear IFW
	F1-7	46	10	66	3	2.9	Moderate swirling
	F1-8	46	10	88	3	2.5	Weak swirling
F2: Varying the diameter of the fuel trays	F2-1	20	5	14	0.5	1.9	Moderate swirling
	F2-2	26	5	14	0.7	2.3	A clear IFW
	F2-3	46	10	33	5	3.3	A clear IFW

Table 2: Summary of tests F1

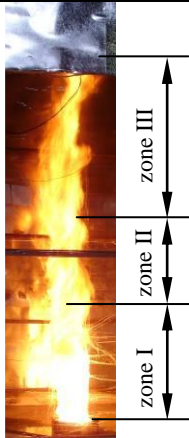
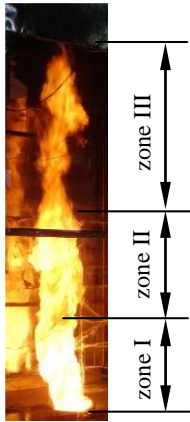
Test No.	F1-1	F1-2	F1-3	F1-4	F1-5	F1-6	F1-7	F1-8
Vertical gap d (cm)	1.3	5.5	11	22	33	44	66	88
IFW	IFW not created	Longer flame height but IFW not created	Unstable swirling, with flame stretched up	IFW created, but not stable	IFW created with three zones	IFW created with three zones	IFW created but not stable	IFW created occasionally
Combustion time (s)	430	400	281	228	202	190	190	330
Maximum flame height (m)	1.5	1.8	3.2	3.5	3.8	3.8	3.6	3.3
Mean flame height f_m (m)	1.3	1.5	2.3	2.9	3.2	3.1	2.9	2.5
Photographs captured								

Table 3: Experiment results of the test F2 on varying the fuel tray diameter

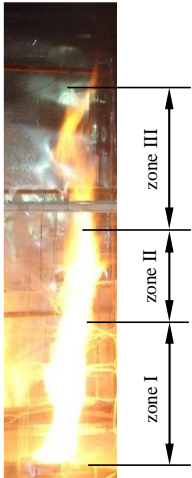
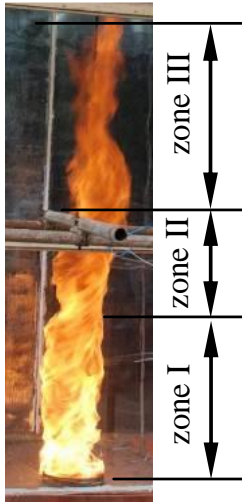
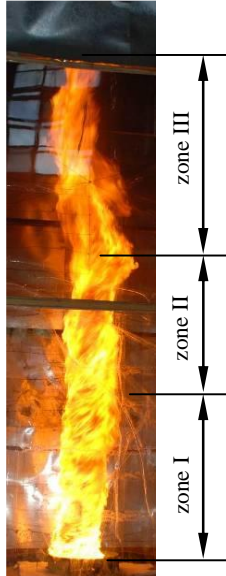
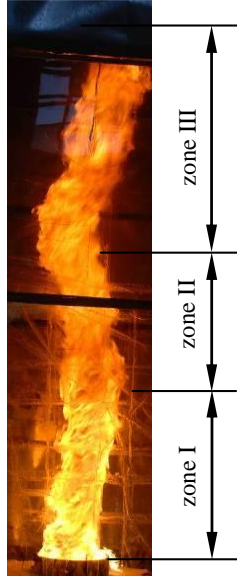
Test No.	F2-1	F2-2	F2-3(1)	F2-3(2)
Diameter of the fuel tray (cm)	20	26	46	46
Vertical gap d (cm)	14	14	33	33
Burning process observed	An IFW was clearly observed, but flame jumping up and down	A stable IFW	A stable IFW	A stable IFW
Burning duration (s)	458	171	305	308
Mean flame height f_m (m)	1.9	2.3	3.3	3.3
Photographs captured				

Table 4: Estimation of heat release rates of IFW

Test	Mass loss rate \dot{m}'' [kg/(m ² · s)]	Effective heat of combustion $\Delta H_{c, \text{eff}}$ [kJ/kg]	Empirical constant $k\beta$ [m ⁻¹]	Diameter of fuel tray D [m]	Heat release rate \dot{Q} [kW]	Remarks on heat release rate
Case 1	—	—	—	0.46	200	\dot{Q} was measured by burning 2 liters gasoline in open air.
Case 2	—	—	—	0.46	225	\dot{Q} was measured by burning 3 liters gasoline in open air.
Case 3	—	—	—	0.46	350	\dot{Q} was measured by burning 4 liters gasoline in the fire room.
Free burning	0.055	43700	2.1	0.46	247.3	\dot{Q} was estimated by equation (1) with recommendation of the mass burning rate in literature.
F2-3	Stage I	0.0620	39800	2.1	253.9	\dot{Q} in stage I was estimated by equation (1) with mass burning rate measured by experiment.
	Stage II	0.0867	39800	2.1	355.0	\dot{Q} in stage II was estimated by equation (1) with mass burning rate measured by experiment.
	Stage IV	0.1156	39800	2.1	473.4	\dot{Q} in stage IV was estimated by equation (1) with mass burning rate measured by experiment.